Shuttlecock aerodynamics

Alison J. Cooke

EDC, Department of Engineering, Cambridge University, Trumpington Street, Cambridge CB2 1PZ, UK

Abstract

Badminton is as popular as lawn tennis (when 'popular' is defined by the number of adults who play the game). Indeed, the origin of the game, played with a feather shuttlecock, in the mid-19th century is said to predate lawn tennis. The invention of the cheaper, more durable synthetic shuttlecock in the 1950s gave the game a wider appeal. Yet, manufacturers have still to produce a synthetic shuttlecock that exactly mirrors the flight of the feather shuttlecock during the game of badminton, a goal they have striving to reach for over 40 years.

This paper describes experiments which were devised to understand the flow regime around a shuttlecock and to accurately determine a data set of aerodynamic coefficients for selected feather and synthetic shuttlecocks. The drag, lift and pitching moment coefficients were measured for a range of Reynolds Numbers (based on maximum skirt diameter) selected to cover most velocities reached in a badminton game; $13\,000 < Re < 190\,000$ (3 to 44 m s^{-1}). The results form part of a wider programme of research which examined the differences between feather and synthetic shuttlecocks and ultimately led to a new product.

Keywords: aerodynamic, badminton, drag, lift, pitching moment, shuttlecock

Nomenclature

C_d	Aerodynamic drag coefficient
C_l	Aerodynamic lift coefficient
C_m	Aerodynamic pitching moment
D	Drag force
d	Maximum diameter of shuttlecock skirt
F	Force applied across strain gauge load cell
g	Gravitational acceleration
H	Length of shuttlecock
L	Lift force
M	Aerodynamic pitching moment
m	Shuttlecock mass
$m_{buoyancy}$	Mass equivalent to buoyancy force on shuttlecock immersed in water

Correspondence address:
Dr A.J. Cooke, Engineering Design Centre, Department of
Engineering, Cambridge University, Trumpington Street,
Cambridge CB2 1PZ.
Tel.: +44 1223 332742, Fax: +44 1223 332662.
E-mail: ajc18@eng.cam.ac.uk

m_{eff}	Effective mass of shuttlecock immersed in water
P	Force applied axially on strain gauge load cell
S	Square of maximum skirt diameter
T_0	Moment applied to strain gauge load cell at position X_0
V	Shuttlecock velocity
V_{term}	Shuttlecock terminal velocity relative to water
x_0	Distance measured along strain gauge load cell from bearing tip
X_0	Position of application of force F, $x_0 = 15$ mm
α	(Angle of) incidence of shuttlecock
ρ	Air density
ρ_l	Density of liquid

Introduction

Badminton as it is known today seems to have originated from 'shuttlecock and battledore' in the 1860s, probably at Badminton House in Avon. The present formal rules for the game were laid down in 1893 (when the Badminton Association of England was formed), and they evolved around the characteristics of the feather shuttlecock. Some rules have changed since then.

Although the original feather shuttlecock design used for badminton can be traced to the mid-19th century, the modern day shuttlecock form was established around 1910; before then it was more barrel shaped. The hand-manufactured feather shuttlecock was the only available badminton projectile until the 1950s, when the development of injection moulding as a manufacturing process had advanced enough to facilitate the production of synthetic shuttlecocks. Synthetic shuttlecocks are more durable and hence cheaper to use. This development increased the popularity of the game as more people could afford to play it. Indeed, in the decade from 1983 to 1993, badminton was the most popular racket sport, despite newly arrived squash and well-established lawn tennis (Taylor & Haake 1998). The most recent results from the same survey estimated that 2% of the adult population (16-years-old and over) regularly play badminton, compared to 2% for tennis and 1% for squash.

So what will players be using for shuttlecocks in the future? In March 1994 The New Scientist (Cooke *et al*. 1994), reported that "within

18 months a new generation of shuttlecocks with carbon feathers could transform players' attitudes." Whilst the timescale for such radical new product development was ambitious, it is not out of the question that shuttlecocks may indeed be manufactured in the future with the use of carbon fibre technology. However, top class players still prefer the feather shuttlecock and consequently these are used in all major badminton competitions. These players believe that the synthetic shuttlecock still does not behave like a feather shuttlecock.

This paper examines the flow regime around the shuttlecock and, by measurement and comparison of the aerodynamic design data sets for feather and synthetic shuttlecocks, discusses some of the major design features which probably explain this perceived difference in flight behaviour.

Shuttlecock selection for research

There is a large variety of shuttlecocks available in shops today, each of which is marketed as having advantages over the others. The shuttlecocks selected for this research were all manufactured by Carlton (Saffron Walden, UK), who provided access to details of manufacturing constraints, player opinion and previous shuttlecock design and development. Two shuttlecocks were analysed: a feather shuttlecock and a synthetic shuttlecock.

The feather shuttlecock was chosen as a control in order to establish the aerodynamic characteristics of a recognized high performance product
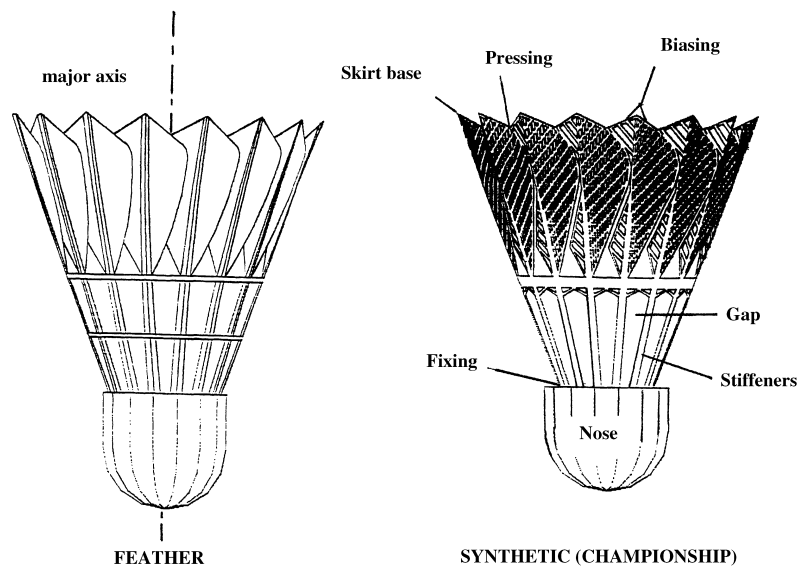
Figure 1 Shuttlecock selection.

Table 1 Shuttlecock dimensions

	Shuttlecock Model	
	Feather	Championship
Skirt diameter, d (mm)	66.0	65.5
Shuttlecock length, H (mm)	86.0	81.5

defining the badminton game. A Carlton Championship was selected as a popular synthetic shuttlecock for comparison with the feather product. The Championship was designed to simulate a feather shuttlecock, both aesthetically and in flight behaviour. (It was also designed to have a high spin/rotation rate about its major axis, similar to the feather shuttlecock.) These shuttlecocks are shown in Fig. 1, with representative dimensions given in Table 1. Both shuttlecocks rotate about the major axis in flight. In this research, all measurements were taken when the shuttlecocks had reached steady state rotation, i.e. the maximum rotation achieved. Further work on the spin dynamics can be found in Hubbard & Cooke (1997).

Flow regimes

The shuttlecock is a bluff body and, as such, the predominant drag regime is base drag. Base drag strongly depends on the base pressure which, in turn, depends on the form of the wake behind the body. A full literature review and discussion on flow over 2D and 3D bluff bodies relating to the shuttlecock is given in Cooke (1992).

Three techniques were adopted to examine the general flow regime around the shuttlecock: smoke flow visualization; pitot-static pressure measurements in wake traverses giving radial velocity profiles and surface static pressure measurements in solid models.

Two features of the shuttlecock of particular note and how these affect the flow regime and drag are discussed here; namely, the skirt porosity and the air jet emerging along the major axis of the shuttlecock (Fig. 1).

Air jet

Static pressure measurements for a full scale solid wooden shuttlecock model suggested that the flow over a shuttlecock separates over the nose and re-attaches on the skirt. This is fully described in Cooke (1992). However, Figs 2 and 3 from the smoke flow visualization experiment for the synthetic (Championship) and feather production shuttlecocks at Re = 4400 ($v = 1$ m s^{-1}), shows that air flows *through* the gap in the shuttlecock skirt.
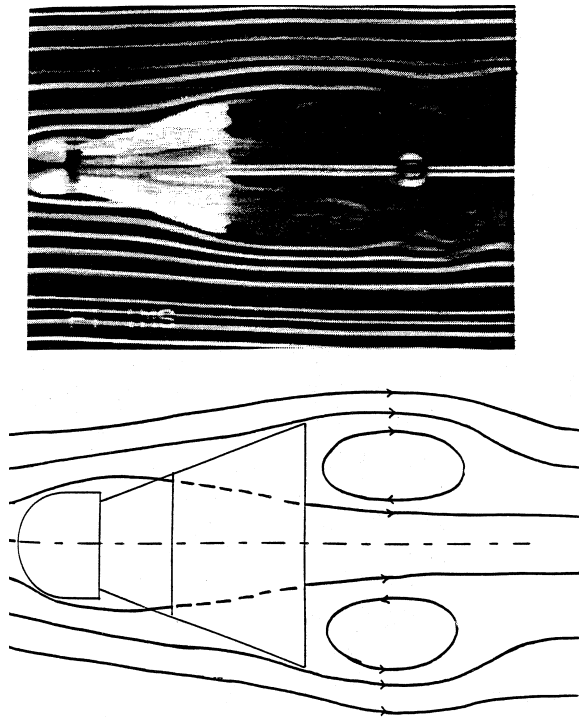
Figure 2 Smoke flow over feather shuttlecock at Re = 4400 ($v = 1$ m s^{-1}).

Figure 3 Smoke flow over championship shuttlecock at Re = 4400 ($v = 1$ m s^{-1}).

This flow leads to a jet of air along the axis of the shuttlecock.

The radial profiles of axial wake velocity confirmed that there is a strong jet passing through the centre of the wake of both shuttlecocks and that, behind the more solid part of the skirts, there is a stagnation area. As was seen by observing the accumulation of smoke behind the feathers, this stagnation area seems to be more severe in the case of the Feather shuttlecock where the feathers present a more complete blockage.

The jet of air through the Feather shuttlecock interacts with the outer flow to produce an unsteady and irregular wake pattern. The outer flow tends to curl inwards towards the shuttlecock axis, whereupon it meets the fast-moving jet of air which tends to curl outwards into the stagnation area behind the feathers. Where the two flows meet, an unsteady flow is produced which is then dissipated downstream. Unlike in the flow over a 2D bluff body (Maull 1978), no strong, regular vortex pattern

emerges. Therefore, it is unlikely that the air jet (or base bleed) emerging along the centre line of the shuttlecock reduces the drag in the same way that it would in the case of a 2D bluff body. Indeed, the air jet was found to increase the drag on the shuttlecock, similar to the effect described by Calvert in his study of flow regimes of solid and porous cones (Calvert 1967). In short, the air jet emerging along the axis of the shuttlecock entrains the wake air, reducing the wake pressure and hence increasing the drag.

Skirt porosity

In addition to the jet of air passing through the gap in the shuttlecock skirt, the synthetic shuttlecocks also exhibit a certain amount of skirt porosity. Figure 3 shows the high level of skirt porosity for the synthetic shuttlecock. The air can be seen *bleeding* through the skirt (the upper half of the shuttlecock wake in the figure). Unlike the synthetic shuttlecock, the Feather shuttlecock has little
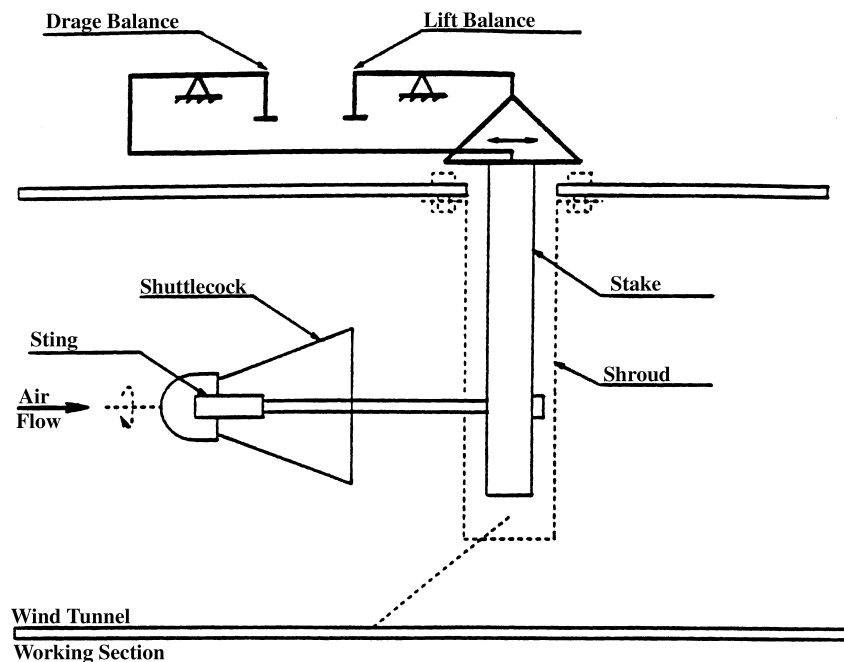
Figure 4 Drag balance experiment.

or no skirt porosity other than the gap. Consequently, the air strikes the feathers and is deflected over them. Even though the synthetic shuttlecock may appear to have more base bleed than the feather shuttlecock, because of its skirt porosity, there will be no drag reduction because there is no strong vortex structure.

Drag coefficient measurement

This section describes the experimental determination of the aerodynamic drag coefficient using a mechanical drag balance and a terminal velocity technique.

Wind tunnel experiment with mechanical drag balance

The drag measurements for the shuttlecocks were carried out in a low speed wind tunnel (Fig. 4), capable of a maximum airspeed of 45 m s^{-1}.

The wind tunnel balance was originally built to measure the drag, lift and pitching moment of aerofoils; measuring drag forces in the range 0–7 N. The maximum system error was 0.02 N which gave a high percentage error in the drag

results at low velocities (Re < 40 000). The terminal velocity technique was developed as an alternative experiment for this low velocity region and will be described in the following section.

A sting was designed to hold the shuttlecock parallel to the airstream. It contained a low friction bearing at its tip to allow free rotation of the shuttlecock.

To eliminate the necessity of measuring a stake drag tare, a shroud was inserted over the stake. The shuttlecock drag was then measured directly from the drag balance.

Each shuttlecock model was mounted on the sting and the drag was recorded for the shuttlecock once it had reached a steady rotation. The drag coefficients were calculated using Equation 1.

$$C_d = D / \tfrac{1}{2} \rho V^2 S \qquad (1)$$

where S is based on maximum skirt diameter.

The results are presented in Fig. 5 for the feather and synthetic shuttlecocks. A full discussion on the blockage effect and system errors, and how these were measured, is given in Cooke (1992).

FEATHER: Cd v Re

Synthetic (Championship): Cd v Re
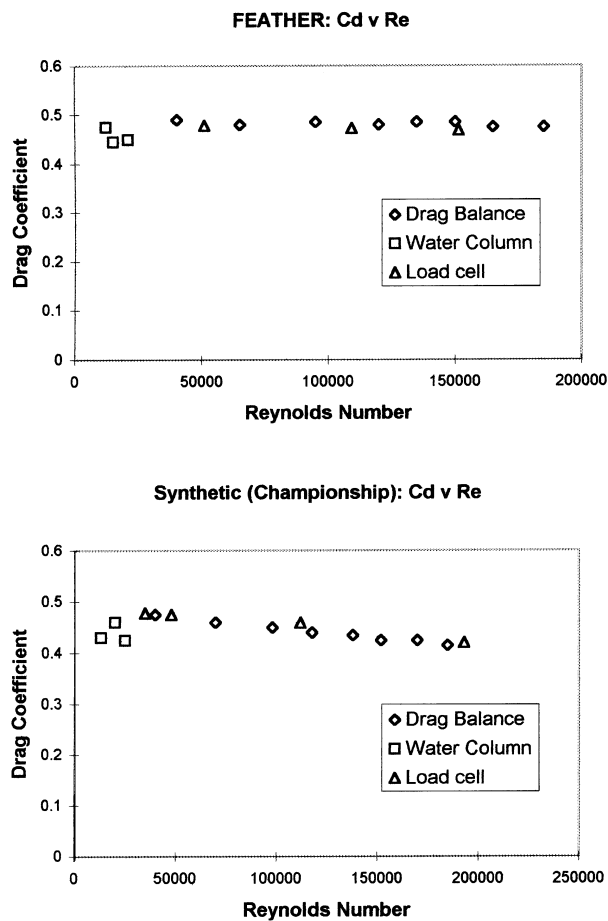
Figure 5 Drag coefficients vs. Reynolds Number.

Terminal velocity experiment for drag measurement

A terminal velocity experiment was devised to give alternative results to the wind tunnel experiment at low Reynolds Numbers (13 000 < Re < 30 000). In this range large errors existed in the wind tunnel experiment.

In this experiment shuttlecocks were dropped through a liquid medium and the terminal velocity was measured by using a laser beam system (Fig. 6).

The equation of motion for a fully submerged shuttlecock falling vertically in a liquid is:

$$mv\frac{dv}{dy} = m_{eff}\boldsymbol{g} - \tfrac{1}{2}C_dS\rho_l v^2 \qquad (2)$$

where m_{eff} is effective mass, defined as $m_{eff} = m - m_{buoyancy}$.

At terminal velocity, $dv/dy = 0$, giving the following expression for terminal velocity:

$$v_{term} = \sqrt{\frac{2m_{eff}\boldsymbol{g}}{\rho_l C_d S}} \qquad (3)$$

The kinematic viscosities of several liquids were considered in order to achieve the desired range of Reynolds Number, but water proved to be the most convenient medium. The Reynolds Number was controlled by varying the shuttlecock terminal velocity. This was achieved by varying the water temperature to adjust its kinematic viscosity and by adjusting the mass of the shuttlecock.

Equations 2 and 3 were used to calculate the depth at which the shuttlecock would reach terminal velocity. If $m = 0.04$ kg, $\rho_l = 991$ kg m^{-3}, $C_dS = 0.002$, $v = 0.99\, v_{term}$, then $y = 0.08$ m. The height of the water above the laser beams was greater than this value to ensure that the terminal velocity was attained before the shuttlecock passed through the first laser beam.

The drag on the shuttlecock at terminal velocity was equal to its effective weight (allowing for the buoyancy effect). The effective mass was measured by weighing the submerged shuttlecock on a spring balance.

Variation of the shuttlecock mass enabled variation of the terminal velocity and, therefore, Reynolds Number. To achieve this, the centre of the shuttlecock noses were drilled out and lead weights inserted.

Equation 3 was used to calculate the value of C_d at each Reynolds Number. A set of readings for the feather and synthetic shuttlecocks was taken at ambient temperature (approx. 17°C).

The Reynolds Number was varied by changing the water viscosity. The viscosity was increased by decreasing the water temperature using ice. The ice was left in the column overnight in order to establish a homogeneous temperature of approximately 4°C. The results are shown in Fig. 5. All errors are fully discussed in Cooke (1992).
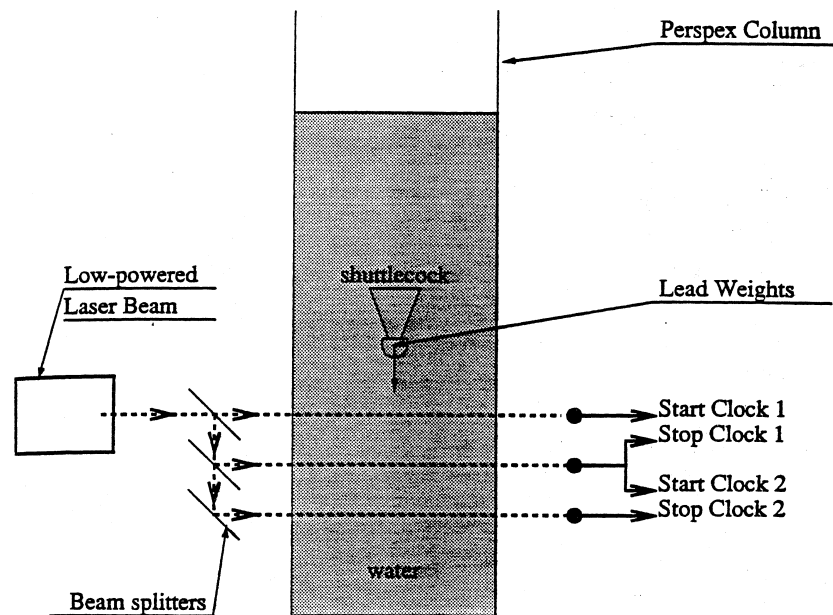
Figure 6 Water column experiment.

In principle, C_d for Re > 30 000 could be measured by increasing the temperature of the water and hence decreasing the viscosity. However, this was not necessary as the wind tunnel experiment was accurate for most of this range.

Analysis of skirt deformation

The skirts of the synthetic shuttlecocks were suspected of deforming at high speeds. The feather shuttlecock is inherently more stiff as the spines of the feathers are tubular, which implies smaller deformations for the feather shuttlecocks at high speeds. It was necessary to verify whether there was skirt deformation in the synthetic shuttlecocks at high speeds and, if so, what effect this was having on the drag coefficients. The verification was carried out using a video camera and an image processing system as described below.

A Panasonic F10 CCD camera and system kit were erected alongside the working section to film the shuttlecock during the drag measurements. A strobe effect shutter of 1/1000 s was used to minimize blurring. A PC-based image processing system was used to determine skirt diameter deformation at high Reynolds Number (Re = 165 000, $v = 38$ m s^{-1} approx.).

Measurement of lift and pitching moment coefficients

To enable a computer prediction of the angular response of the shuttlecock, particularly at the apex of its trajectory, data sets of the lift and pitching moment coefficients were required in addition to the drag coefficient. A multicomponent strain gauge load cell was designed for these measurements over a range of incidences (0–30°). It incorporated 8 strain gauges and was suitable for wind tunnel use. The design calculations were based on strain gauge theory described by Potma (1967). The load cell is shown in Fig. 7.

The load cell incorporated three Wheatstone bridge circuits: two full bridges, measuring forces P and F, and one half bridge circuit, measuring the bending moment, T_0.

Wind tunnel experiments

The experimental set up was similar to previous experiments (Fig. 4), but the sting was replaced by the load cell. The bearing of the load cell was pushed into the nose of the shuttlecock to a depth of 5 mm. The load cell was then connected to the data processing equipment via cables through the tunnel floor downstream of the shuttlecock.
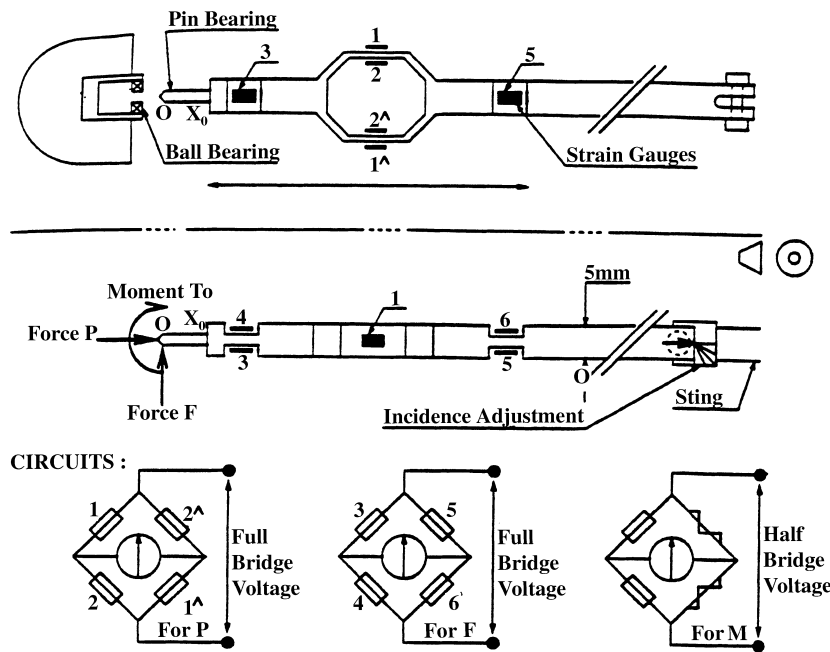
Figure 7 Strain gauge load cell.

The loads on feather and synthetic shuttlecocks were measured at incidences of 0, 10, 15, 20, 25 and 30° over a range of Reynolds Number 50 000 < Re < 160 000 (11 m s^{-1} < v < 37 m s^{-1}). In all cases, the shuttlecock was allowed to rotate on the sting but it was found that at higher incidences (> 30°) the shuttlecock did not freely rotate (due to restriction by the sting). In the case of the synthetic shuttlecock, this caused skirt deformation.

Results

A computer program used the strain gauge measurements from The load cell to calculate P, F and T_0 for the shuttlecock. These were then used to compute the lift, drag and pitching moment coefficients using the equations below. The frame of reference was transferred to the centre of gravity. This later facilitated the analysis of the equations of motion when the shuttlecock was treated as a body which rotated about its centre of gravity. The coefficients are used to predict the shuttlecock motion.

$$\text{Lift}, L = F \cos \alpha - P \sin \alpha \qquad (4)$$

$$\text{Drag}, D = F \sin \alpha + P \cos \alpha \qquad (5)$$

$$\text{Pitching Moment}, M = T_0 + F x_0' \qquad (6)$$

where x_0' is the distance from position O on the load cell to the centre of gravity. The lift and pitching moment coefficients were then calculated from:

$$C_1 = L / \tfrac{1}{2} \rho V^2 S \quad \text{and} \quad C_m = M / \tfrac{1}{2} \rho V^2 S H. \qquad (7)$$

The drag coefficient results in Fig. 5 suggest that the errors in the calculated forces due to the equipment are not substantial. In the figure it can be seen that the C_d values agree closely with the results from both the wind tunnel and terminal velocity.

The drag, lift and pitching moment coefficients are shown in Figs 8, 9 and 10 for a range of Reynolds Number and at various constant incidences. In these figures, the lift, drag and pitching moment coefficients are plotted vs. incidence at Re = 53 000 and Re = 145 000 (equivalent to approximately 11 and 32 m s^{-1}). These aerodynamic coefficients were used in the computer program to predict the angular response of the shuttlecock.
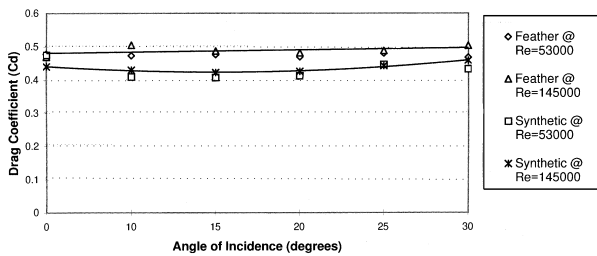
Figure 8 Drag coefficients vs. incidence (load cell).
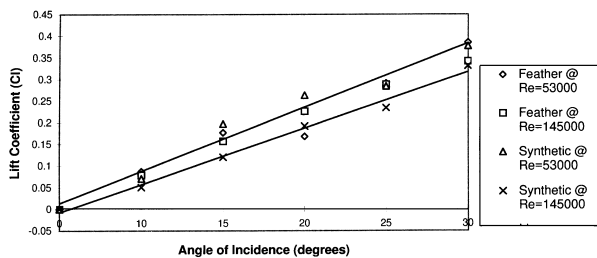
Figure 9 Lift coefficients vs. incidence (load cell).
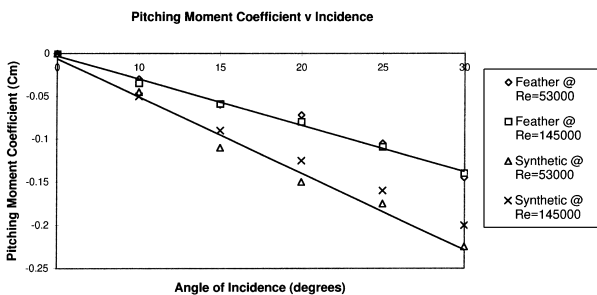
Figure 10 Pitching moment coefficients (load cell).

Discussion

In the following, the values of the aerodynamic coefficients for the production shuttlecock models are compared. The majority of the results are presented in terms of Reynolds Number based on the maximum skirt diameter ($0 < Re < 200\,000$ corresponds to $0 < v < 45$ m s^{-1}), covering the range of velocities found in a typical badminton game.

The drag coefficients

Figure 5 shows the drag coefficients for each shuttlecock from the three experiments. The feath-er shuttlecock has a constant drag coefficient (at approx. 0.48) over the whole range of Reynolds Number ($13\,000 < Re < 190\,000$). The drag coefficients for the synthetic shuttlecock decrease with increasing Reynolds Number. The lower values of C_d from the water column experiment are explained by the variation in skirt diameter between different shuttlecocks of the same model. (A 2-mm difference in diameter can effect the drag coefficient by 0.03.) The drag coefficients for both shuttlecock models in Fig. 5 show that the coefficients are approximately equivalent and constant (at approx. 0.48) up to a Reynolds Number of about 70 000 (or 16 m s^{-1}). This result is both encouraging and surprising.

It is encouraging because the development of the synthetic shuttlecock has aimed to reproduce the flight characteristics of a feather shuttlecock. This result proves that, up to a Reynolds Number of 70 000, the drag characteristics for the synthetic shuttlecock match those of the feather shuttlecock.

The similarity between the drag characteristics of the synthetic and feather shuttlecocks is surprising because it is generally found that the drag coefficient of an object decreases with increasing porosity, as described in Hoerner (1965). Synthetic shuttlecocks are more porous than the feather shuttlecocks and therefore it might be expected that its drag coefficient were smaller. If the synthetic (the most porous shuttlecock) and the feather shuttlecock are compared in Fig. 5 it can be seen that the drag coefficients are equivalent up to a Reynolds Number of approximately 70 000. Therefore, the shuttlecock porosity does not seem to be affecting the drag characteristics in the usual manner. As mentioned earlier, the predominant feature of the flow over and through the shuttlecock is the air jet and this dominates any skirt porosity effects.

The jet of air would have a 'jet-pump' action similar to the air flowing over the shuttlecock, as reported by Hoerner (1950). The jet of air entrains the dead air in the wake, causing a further reduction in the static pressure in the shuttlecock stagnation area.

Skirt deformation

Above a Reynolds Number of 70 000 the drag co-efficient decreases for the synthetic shuttlecock and remains constant for the feather shuttlecock. It has long been suspected that one of the disadvantages of the synthetic shuttlecock is that the skirt material flexibility causes the skirt to deform during flight.

The images processed for analysis of skirt deformation at high Reynolds Numbers showed that the synthetic shuttlecock (considered to be the most flexible of the synthetic models) did experience skirt deformation at high Reynolds Numbers – in this case a diameter reduction of about 1 mm at app-roximately 165 000 (velocity about 38 m s^{-1}). Conversely, the feather shuttlecock has no measurable skirt deformation at the same Reynolds Number.

It is interesting to note that, of all the shuttlecocks examined, those which demonstrated the greatest reduction in drag coefficient were those which had the deepest pressing during the manufacturing process (i.e. the deviations from a circle around the skirt base were largest). It is highly probable that the deep pressing is the cause of a 'concertina' effect which facilitates the closing up of the skirt at high Reynolds Numbers.

Drag at incidence

Figure 8 indicates that the drag coefficients are fairly constant over the range of incidence covered by the experiment.

Comparison with previous work

The drag coefficient data from three other sources, Wichers Schreur (unpublished data), Ward-Smith & Gibson (Unpublished data) and Peastrel *et al.* (1980), generally agree with this work even though they all consider shuttlecocks of different makes (all measurements were normalized to account for area differences, i.e. diameter variations).

Wichers Schreur measured the drag on several shuttlecock models. A drag coefficient of 0.5 was found for an RSL feather shuttlecock as opposed to a Carlton feather shuttlecock which was used in this work. Even so, both sets of data are in agreement within experimental error. Wichers Schreur used a technique for measuring the stake drag tare and this is more susceptible to errors than the shrouded experimental technique. This probably helps to explain the scatter of his data points.

Ward-Smith & Gibson reported a constant drag coefficient of 0.51 (based on the frontal area) for a Moroe Seisakusho Company Ltd. feather shuttlecock. This result has been converted to a drag coefficient based on skirt area. Again, this favourably agrees with the data from this work on the Carlton Feather shuttlecock.

Lift and pitching moment coefficients

The load cell experiment measured the drag, lift and pitching moment coefficients for the shuttlecocks at various incidences over the range of Reynolds Number, 50 000 < Re < 160 000 (12 m s^{-1} < v < 35 m s^{-1}).

Lift

Figure 9 shows the lift coefficients plotted vs. incidence for both shuttlecocks at Re = 53 000 and Re = 145 000 (the minimum and maximum Reynolds Numbers tested). At 0° incidence, it is reasonable to apply a no-lift condition for an axi-symmetric bluff body (e.g. fig. 33 in Hoerner 1965 and fig. 9 in Bostock 1974).

As expected, Fig. 9 shows an approximately linear increase in lift coefficient with incidence. The data for the feather shuttlecock shows very close agreement between the low and high Reynolds Numbers. There is a smaller increase in lift coefficient with incidence for the synthetic shuttlecock at the higher Reynolds Number, most probably explained by decreased frontal area. Variations in this effect between the shuttlecocks may be partly due to differences in skirt porosity which change the effective frontal area. The lift coefficients for the respective shuttlecocks are similar.

The feather shuttlecock reaches a C_l of 0.38 at an incidence of 30° and the synthetic shuttlecock has similar characteristics, reaching a C_l of approximately 0.3 at an incidence of 30°.

Pitching moment

As can be seen in Fig. 10, the pitching moment is always negative and is thus a restoring moment. Hence, the shuttlecock is always stable. The pitching moment coefficients (based on the length of the shuttlecock) approximately follow the same trends as the lift coefficients in both figures.

Conclusions

Little technical information is available on the subject of shuttlecocks. However, in this research, shuttlecock aerodynamics was investigated by:

- considering relevant literature on 2D and 3D bluff bodies;
- performing flow visualization experiments to determine flow regimes;
- comparisons of aerodynamic coefficient measurements for synthetic and feather shuttlecocks;
- discussing particular design features affecting shuttlecock aerodynamic coefficients.

It was found that:

- the shuttlecock is a bluff body and the predominant drag mechanism is base drag.
- Increased porosity does not necessarily reduce the drag coefficient. The introduction of the gap in the shuttlecock skirt was found to increase drag coefficient because of the strong axial air jet, producing a *jet-pump* effect.
- The drag coefficients of the feather and synthetic shuttlecock were approximately constant (at 0.48) and equivalent up to Reynolds Numbers of 70 000 (16 m s^{-1}). Above Re = 70 000, the drag coefficient decreased for the synthetic shuttlecock and stayed constant for the feather.
- It was shown that this decrease in drag coefficient was due to a reduction in frontal area caused by skirt deformation.

- The lift coefficients for both shuttlecocks increase with increasing incidence, reaching values over 0.3 at 30° incidence.
- The pitching moment coefficient measurements for both shuttlecocks suggested that the aerodynamic centre is always behind the centre of gravity, i.e. the shuttlecocks are stable at all times.

These conclusions were used in the development of a new synthetic shuttlecock product, as discussed in Dixon & Cooke (1995) and Cooke (1996).

Acknowledgements

References

Bostock, B.R. (1974) *Slender Bodies of Revolution at Incidence*, PhD Thesis, Cambridge University, Cambridge, UK.

Calvert, J.R. (1967) *The Separated Flow behind Axially Symmetric Bodies*, PhD Thesis, Cambridge University, Cambridge, UK.

Cooke, A.J. (1992) *The Aerodynamics and Mechanics of Shuttlecocks*, PhD Thesis, Cambridge University, Cambridge, UK.

Cooke, A.J. (1996) Shuttlecock design and development. *Sports engineering – design and development* (ed. S. J. Haake). Proceedings of the 1st International Conference on the Engineering of Sport. Blackwell Science, Oxford, UK.

Cooke, A.J. & Mullins, J. (1994) The flight of the shuttlecock, *New Scientist*, **1916**, March.

Dixon, J. & Cooke, A.J. (1995) Managing product design: a case study from the consumer sports industry. Product Design Seminar 1995, Teaching Company Directorate.

Hoerner, S.F. (1950) Base drag and thick trailing edges. *Journal of the Aeronautical Sciences*, **17**, 622–628.

Hoerner, S.F. (1965) *Fluid Dynamic Drag*. Hoerner Fluid Dynamics, Midland Park, NJ, USA.

Hubbard, M. & Cooke, A.J. (1997) Spin dynamics of the badminton shuttlecock. Biomechanics Conference, Tokyo University.

Maull, D.J. (1978) Mechanisms of two and three-dimensional base drag. *Symposium on Aerodynamic Drag Mechanisms of Bluff Bodies and Road Vehicles*. Plenum Press, New York, NY, USA.

Peastrel, M., Lynch, R. & Armenti, A. Jr (1980) Terminal velocity of a shuttlecock in vertical fall. *American Journal of Physics*, **48**, 511.

Potma, T. (1967) *Strain Gauges: Theory and Application*. Philips Paperbacks, Eindhoven, The Netherlands.

Taylor, P. (1998) The economics of the sports products industry. *Sports Engineering – Design and Development* (ed. S.J. Haake). Proceedings of the 2nd International Conference on the Engineering of Sport. Blackwell Science, Oxford, UK.